Journal of Polymer Research (2022) 29:481
https://doi.org/10.1007/s10965-022-03327-5

ORIGINAL PAPER

Graphene nanoplate incorporated Gelatin/poly(2-(Acryloyloxy) ethyl trimethylammonium chloride) composites hydrogel for highly effective removal of Alizarin Red S from aqueous solution

Fatma Ozsoy[1] · Batuhan Ozdilek[1] · Alper Onder[2] · Pinar Ilgin[3] · Hava Ozay[2] · Ozgur Ozay[4]

Received: 24 July 2022 / Accepted: 19 October 2022 / Published online: 26 October 2022

Abstract

The increasing water pollution day by day has increased the importance of developing new adsorbent materials. In this study, composite hydrogel containing gelatin, [2-(Acryloyloxy)ethyl] trimethylammonium chloride (AETAC) and Graphene Nanoplate (GNPt) was developed as an adsorbent for the removal of dyes from wastewater. Fourier Transform Infrared Spectrophotometer, Scanning Electron Microscope, X-Ray Diffractometer results confirmed the crosslinked polymer structure of Gelatin/p(AETAC)/GNPt composite hydrogel (Gel 5). In addition, equilibrium swelling ratio, which is a parameter affecting the adsorption behavior, was 48.22 g_{water} /g_{gel}. The adsorption behavior of Alizarin Red S anionic dyestuff on composite hydrogel from aqueous solutions was investigated under various experimental conditions such as initial dye concentration of solution, amount of adsorbent, contact time, pH of solution, temperature of solution. ARS dye adsorption on composite hydrogel is consistent with Pseudo-Second-Order kinetic model and Langmuir isotherm with max adsorption capacity of 649.35 mg/g. The composite hydrogel with high mechanical strength has high dye removal ability in the ranging pH from 4 to 8. Therefore, it can be said that Gelatin/p(AETAC)/GNPt composite hydrogel has a substantial potential for the removal of anionic dyes from wastewater in a wide pH range.

Keywords Graphene nanoplate · Composite hydrogel · Alizarin Red S · Adsorption · Isotherms · Kinetics

Highlights

- Gelatin/p(AETAC)/GNPt composite hydrogel containing graphene nanoplate was prepared successfully.
- ARS anionic dye adsorption of composite hydrogel was investigated.
- The composite hydrogel had a high ARS dye removal ability in a wide pH range.
- The maximum dye adsorption capacity of composite hydrogel can reach 649.35 mg/g according to the Langmuir isotherm.
- It was determined that porous composite hydrogels with high anionic dye adsorption and mechanical strength, which can be used in a wide pH range, are good adsorbent candidates.

✉ Alper Onder
alperonder@outlook.com

[1] School of Graduate Studies, Department of Bioengineering, Çanakkale Onsekiz Mart University, Çanakkale, Türkiye

[2] Laboratory of Inorganic Materials, Department of Chemistry, Faculty of Science, Çanakkale Onsekiz Mart University, Çanakkale, Türkiye

[3] Department of Chemistry and Chemical Processing Technologies, Lapseki Vocational School, Çanakkale Onsekiz Mart University, Çanakkale/Lapseki, Türkiye

[4] Department of Bioengineering, Faculty of Engineering, Çanakkale Onsekiz Mart University, Çanakkale, Türkiye

Introduction

With the increasing population and developing industrial diversity, large volumes of industrial and domestic wastes that may cause environmental problems have been generated. Synthetic dyes are among the most common hazardous and dangerous contaminants [1]. Alizarin Red S (ARS) dye is a synthetic dye commonly used in the textile industry and for colouring biological materials [2]. ARS dye with high thermal, optical and physicochemical stability may cause adverse effects on marine life by affecting photosynthesis [3]. It also causes significant health problems in humans, such as mutagenic effects, skin disorders, vision defects, and allergies [2]. Many synthetic dyes, which have a wide range of uses, have been separated from wastewater for a sustainable environment and life. Many methods such as electrochemical oxidation [4], membrane filtration [5], coagulation [6], photocatalytic process [7], and adsorption [8] have been reported to separate synthetic dyes from aqueous environments. The most successful, non-expensive, productive, and preferred of these processes is the separation of synthetic dyes by the adsorption method [9, 10]. With an adsorbent

with biocompatible, high surface area, high dye recovery, and reusable properties, highly polluting dye can be removed from wastewater, dye can be recovered and quality clean water can be obtained [3]. In recent years, various absorbent materials such as nanospheres [11], nanotubes [12], metal organic frameworks [13], hydrogels [14], and composite hydrogels [15] have been introduced to the literature. Among these, composite hydrogels prepared using various materials such as fly ash [15], bentonite [16], montmorillonite [17], graphene oxide [18], which contribute to the improvement of the properties of hydrogels, have attracted the attention of researchers. The materials added to the structure in the preparation of composite hydrogels are known to increase the hydrogel's adsorption ability as well as their structural strength [19]. Gad and Nasef reported that graphene oxide-containing poly(2-acrylamido-2-methylpropane sulfonic acid)/polyvinyl alcohol composite hydrogels could be used as an efficient adsorbent for the removal of basic blue 3 dye from aqueous solutions [20]. In another study, it was reported that the poly(acrylic acid)/laponite nanocomposite hydrogel with high mechanical properties showed a superior adsorption capacity of 3796 mg/g for methylene blue [21]. Graphene-based hydrogels have become even more interesting in recent years for the development of versatile and functional materials [22]. Graphene has been widely investigated from energy to the environment because of its unique properties. It is currently the thinnest and most sturdy material with a large specific surface area [23]. Thanks to the nanopores in composite hydrogels made with graphene nanoplates (GNPt), they have a high amount of adsorption capability [22].

[2-(Acryloyloxy)ethyl] trimethylammonium chloride (AETAC) is a kind of cationic monomer and contains ammonium groups in its structure. It can interact with anionic dyes/drugs thanks to its functional groups and electrostatic effects [24]. Due to the most active groups in the molecular structure such as amino groups, hydroxyl groups and carboxyl groups, the chemical and physical properties of gelatin can be improved [25]. In many studies in the literature, researchers frequently use gelatin due to its superior properties such as biocompatibility [26], immunogenicity, water-solubility, non-toxicity, and biodegradability [27, 28]. However, gelatin hydrogels generally have relatively poor mechanical strength which limits their application in many areas. The physicochemical and mechanical properties of gelatin-containing hydrogels can be improved with various functional materials such as graphene oxide and microfibrillated cellulose [29, 30]. In this way, there is an increasing interest in gelatin-containing composite polymer structures with improved mechanical properties and stability for various application areas.

Here, as far as we know, for the first time, a highly biocompatible mechanical strength composite hydrogel containing GNPt is developed using gelatin and AETAC monomers. The functionality of the successfully synthesized Gelatin/p(AETAC)/GNPt composite hydrogels was demonstrated by the removal of ARS dye. The Gelatin/p(AETAC)/GNPt composite hydrogel was characterized by Fourier Transform Infrared Spectrophotometer, Scanning Electron Microscope, X-Ray Diffractometer analysis, and swelling behavior. It has been shown by studies that the synthesized new Gelatin/p(AETAC)/GNPt composite hydrogel has excellent stability for the removal of anionic dyes from industrial wastewater and has a guiding quality for future studies.

Experimental

Materials and instruments

AETAC (80 wt.% in H_2O) as a monomer, N,N'-methylenebisacrylamide (MBA) as a crosslinker, ammonium persulfate (APS) as an initiator, and N,N,N',N'-tetramethylethylenediamine (TEMED) as an accelerator were obtained from Sigma-Aldrich. Gelatin was obtained from Carlo Erba. Graphene nanoplate (GNpt, Surface area 750 m^2/g) was obtained from Sigma-Aldrich. Dyes (Methyl orange – MO, reactive black 5—RB5, alizarin red S—ARS, safranin O—SO, methylene blue—MB, malachite green—MG) used for adsorption studies were obtained from Sigma-Aldrich, Merck and ISOLAB companies.

Fourier Transform Infrared Spectrophotometer (FT-IR) analysis of Gelatin/p(AETAC)/GNPt composite hydrogels were obtained using a Perkin Elmer spectrum 100 spectrometer (650–4000 cm^{-1}) with ATR apparatus. FEI QUANTA FEG 250 model scanning electron microscope (SEM) was used for the morphology of the composite hydrogel. Composite hydrogel samples were lyophilized before measuring with the SEM device. XRD analysis was completed on GNPt and Gelatin/p(AETAC)/GNPt composite hydrogel using a PANalytical Empyrean model x-ray diffraction (XRD) device in the 5–80 °2Th interval with CuKα (λ = 1.54 Å) radiation. The amount of dye adsorbed by the Gelatin/p(AETAC)/GNPt composite hydrogels was determined by calibration charts using UV–vis spectrophotometry (T80 + UV/VIS Spectrometer, PG Ins. Ltd.). The mechanical compression test of the composite hydrogel was measured with a UniVert (Cellscale biomaterials testing). To determine the effect of pH on dye adsorption, a Hanna brand pH meter was used for the preparation of various pH solutions. All experiments within the study were repeated three times.

Preparation of gelatin/p(AETAC)/GNPt composite hydrogels

Gelatin/p(AETAC)/GNPt composite hydrogel was prepared using the free radical copolymerization method similar to our previous studies [14, 15]. First, gelatin solution was prepared in hot (65 °C) distilled water at a concentration of 20% w/v. Different composite hydrogels were prepared with 100 rpm stirring in 20 ml vial, according to the proportions shown in Table 1. 0.01 g of APS in 100 µL of deionized water was added to initiate gelation. The solution was transferred into pipettes with a diameter of 0.5 cm. Then gelation was followed by temperature control. In the case of overheating, the gelation reaction was kept stable by cooling. After approximately 45 min of gelling, the graphene composite hydrogel was removed by precision cutting the pipette and cutting into 0.5 cm lengths. It was dried in an oven at 40 °C for about 5 h. Graphene composite hydrogels were washed in deionized water for one day to remove soluble oligomer, uncrosslink polymer and unreacted monomers, and the water was changed approximately every 8 h during this process. The washed Gelatin/p(AETAC)/GNPt composite hydrogels were left to dry by being careful not to break down, and after they were dried at room conditions for three days, they were placed in an oven again and dried at 40 °C for approximately 24 h. After these procedures, yield and sol–gel calculations were made for the gels. The formulas used for these calculations are as follows.

$$Yield\ \% = (W_c/W_i) \times 100 \tag{1}$$

$$Gel\ \% = (W_d/W_c) \times 100 \tag{2}$$

$$Sol\ Gel\% = 100 - Gel \tag{3}$$

where, W_c: gel mass dried in an oven before washing in distilled water to remove water soluble part, W_d: gel mass dried in an oven after washing in distilled water to remove water soluble part, W_i: total mass of AETAC, gelatin, MBA, graphene nanoplate.

Swelling characteristic of Gelatin/p(AETAC)/GNPt composite hydrogels

Swelling behaviors and equilibrium swelling ratios of Gelatin/p(AETAC)/GNPt composite hydrogels in deionized water were investigated using gravimetric methods. In this method, firstly, the initial dry mass (W_d) of the Gelatin/p(AETAC)/GNPt composite hydrogel was weighed at room temperature. Each of them was thrown into the swelling media at the determined volumes separately. Swollen composite hydrogel at certain time intervals was removed from the swelling medium. The excess amount adsorbed by the filter paper was taken and swollen composite hydrogel was weighed (W_s). These steps were repeated for all composite hydrogels and times. The equilibrium swelling ratio (ESR, $g_{water}/g_{hydrogel}$) of Gelatin/p(AETAC)/GNPt composite hydrogels was determined using the Eq. (4) [31].

$$ESR = (W_s - W_d)/W_d \tag{4}$$

Adsorption studies

Adsorption behaviors were observed to determine the interactions of the composite hydrogel with anionic and cationic dyes [14]. In the first stage, adsorption studies were carried out for dye selectivity in MO (464 nm), RB5 (596 nm), ARS (516 nm) as anionic dyes and SO (520 nm), MB (663 nm), MG (617 nm) as cationic dyes. Dye solutions prepared in distilled water were measured using a UV–Vis spectrophotometer in a wavelength range of 300–800 nm. (Fig. S1) [32–36]. A linear regression curve was produced from the calibration curve and used to convert dye adsorption to concentration throughout a concentration range. 30 mg of the Gelatin/p(AETAC)/GNPt composite hydrogel (Gel 5) were transferred into 30 mL of each dye solution (250 mg/L) and allowed to equilibrate at 25 °C for 24 h. In the second stage, adsorption studies were carried out at 25, 50, 100, 250, 500, 750, and 1000 mg/L concentrations

Table 1 Chemical ratios used for Gelatin/p(AETAC)/GNPt Composite Hydrogel synthesis

Gelatin/p(AETAC)/GNPt composite hydrogel	AETAC (mL)	Gelatin (20% w/v) (mL)	Graphene (mg)	Gel %	Sol %	Yield %
Gel 1	1	0.1	0	85.16	14.84	93.89
Gel 2	1	0.1	10	85.43	14.57	95.35
Gel 3	1	0.2	10	86.35	13.65	97.96
Gel 4	1	0.1	20	86.59	13.41	97.60
Gel 5	1	0.1	30	87.73	12.27	97.77
Gel 6	1	0.3	10	89.35	10.65	95.99
Gel 7	1	0.4	10	88.61	11.39	95.09
Gel 8	1	0.5	10	88.44	11.56	95.96
Gel 9	1	0	10	87.83	12.17	96.50

MBA (7.3 mg), TEMED (20 µL)

to determine the effect of the initial dye concentration of ARS on the adsorption of the composite hydrogel.

At the same time, temperature (25 °C; 35 °C; 45 °C and 55 °C), amount of adsorbent (0.5 g/L; 1 g/L; 2 g/L; 3 g/L; 4 g/L;) pH (4,5,6,7,8) and contact time (15 min -24 h) parameters affecting dye adsorption were studied within the scope of the study. The equilibrium adsorption capacity (q_e, mg dye/g gel) percent removal ratio (R%) was calculated by considering the concentrations of the dye solutions in which graphene composite hydrogel was added before (C_0) and after adsorption (C_e). For this, Eqs. (5) and (6) below are used.

$$q_e = (C_0 - C_e) \times V/W \tag{5}$$

$$R\% = (C_0 - C_e)/C_0 \times 100 \tag{6}$$

where, V corresponds to the volume of the dye solution (L) and W corresponds to the dry graphene composite hydrogel mass (g) [14].

Desorption studies

To determine the reusability of the Gelatin/p(AETAC)/GNPt composite hydrogel (Gel 5), the adsorption process of 100 mg/L ARS solution at 25 °C and 24 h was performed. Desorption process was carried out by keeping the dye adsorbed composite hydrogel in 0.01 M NaOH medium for 24 h. After desorption, the composite hydrogel was kept in 0.01 M NaCl for 24 h. Then it was prepared for the next adsorption by washing with distilled water for 6 × 8 h. The above adsorption–desorption process was repeated 3 times for the composite hydrogel [37].

Porosity studies

The porosity properties for the Gelatin/p(AETAC)/GNPt composite hydrogel (Gel 5) was investigated using the solvent exchange method [38]. First, graphene composite hydrogels, which were completely dried in an oven, were weighed. Then, it was discarded in the determined volume of ethanol and left for 24 h. Then, graphene composite hydrogels extracted from the solvent were removed from excess ethanol and weighed again. The porosity (%) was calculated by substituting the obtained data in Eq. (7). Porosity tests were performed in triplicate.

$$Porosity = ((M_2 - M_1)/\rho \times V) \times 100 \tag{7}$$

where, M_1 and M_2 represent the mass of the hydrogel before and after absolute ethanol immersion, respectively. ρ and V are ethanol density (0.789 g/mL) and hydrogel volume, respectively.

Result and discussions

Synthesis and characterization of composite hydrogels

Access to water resources is vital important for the continuity of life. One of the most significant pollutants of usable water is synthetic dyes [18]. For this reason, p(AETAC-co-Gelatin)/GNPt composite hydrogels as a new adsorbent material for the treatment of wastewater and sustainable water economy were synthesized using the free radical copolymerization method in the amount of different components (gelatin, GNPt) in Table 1 (Fig. 1a). As can be seen in Table 1, the increase in the amount of GNPt has increased the gelation % and yield % of composite hydrogels. In this case, it can be said that the composite hydrogel crosslinks are supported by graphene nanoplates. At the same time, it was observed that the brittleness of the composite hydrogels was related to the increasing amount of gelatin. It has been reported that the mechanical strength properties of hydrogel systems prepared with gelatin are low [39]. Among the composite hydrogels prepared according to Table 1, Gel 5 had a non-brittle structure.

The variables of the yield calculation (X_1, X_2, X_3) according to the factorial design and the interactions between them were calculated using the signs in Table 2 for the 2^3 factorial and matrix designs. Here, the relationship between the dependent variables (X_1, X_2, X_3) and the independent variable (% yield for hydrogels) was determined using the multiple linear regression method [40]. As a result of the analysis, the following polynomial Eq. (8) was obtained.

$$y = 96.27 + 0.09X_1 + 0.52X_2 + 0.07X_3 + 0.17X_1X_2 - 0.18X_1X_3 - 1.06X_2X_3 + 0.62 + \varepsilon \tag{8}$$

The variables X_1, X_2, X_3 determined here are the total mass of gelatin, graphene, and reacted chemicals, y is the yield percentages of the hydrogels, respectively. The equations and data obtained were formulated in a similar way to the studies in the literature [31].

The FT-IR spectrum of the prepared composite hydrogel (Gelatin/p(AETAC)/GNPt, Gel 5) is given in Fig. 1b. In the FT-IR spectrum, the O–H stretching vibration or N–H stretching vibration of the amide A band of gelatin had a strong peak in the range of 3600 – 3200 cm^{-1}. The C–H

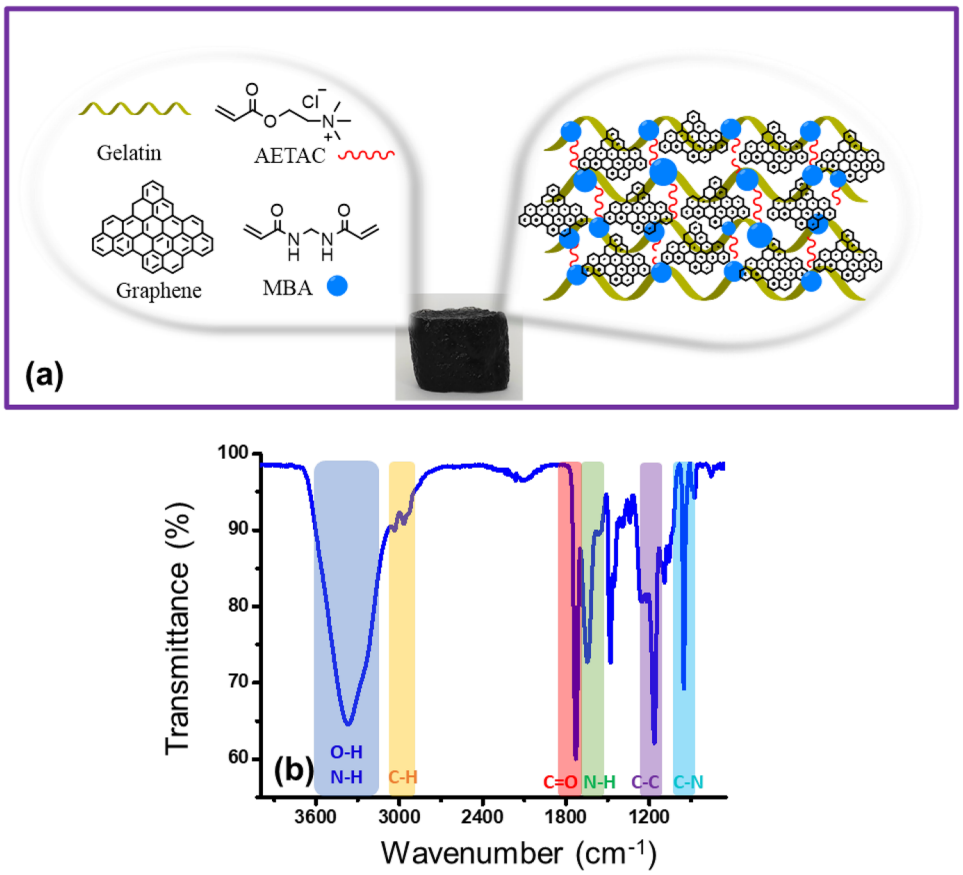

Fig. 1 **a** Illustration of the synthesis scheme and **b** FT-IR spectrum of Gelatin/p(AETAC)/GNPt composite hydrogel (Gel 5)

stretch (3035 – 2956 cm^{-1}) and C = O stretching (1729 cm^{-1}) from the functional groups of gelatin, AETAC, and MBA in the composite hydrogel structure were observed in the spectrum. In addition, the characteristic absorption bands observed at 1646 and 951 cm^{-1} correspond to the N–H stretching in the structure of gelatin and MBA, and the C–N stretching vibration of the quaternary ammonium groups in the structure of AETAC, respectively [14, 41, 42]. Also, C = C aromatic ring stretching band of graphene observed at 1571 cm^{-1}. These results show that the Gelatin/p(AETAC)/GNP composite hydrogel has been successfully obtained.

In the XRD model of GNPt in Fig. 2a, the broad peak at 26.7° and the weak intensity diffraction peaks at 43.5° are assigned to the graphene carbon crystal planes (002) and (100), respectively [43–45]. In the XRD model of Gel 5 in Fig. 2b, the diffraction peaks of GNPt with a value of

Table 2 2^3 full factorial and matrix design for yield optimization of Gelatin/p(AETAC)/GNPt Composite Hydrogels

Independent variables				Independent variables			Dependent variables
Gelatin/p(AETAC)/GNPt	X_1	X_2	X_3	GNPt (g)	Gelatin (g)	TM (g)	Yield %
Gel 2	-	-	-	0,01	0,02	1,08	95.35
Gel 3	+	-	-	0,01	0,04	1,10	97.96
Gel 4	-	+	-	0,02	0,02	1,08	97.60
Gel 5	+	+	-	0,03	0,02	1,08	97.77
Gel 6	-	-	+	0,01	0,06	1,12	95.99
Gel 7	+	-	+	0,01	0,08	1,14	95.09
Gel 8	-	+	+	0,01	0,1	1,16	95.96
Gel 9	+	+	+	0,01	0	1,06	96.50

The (-) and (+) signs indicate low and high levels of a factor, respectively

TM total mass of chemicals involved in the reaction

2θ disappear. This may be a result of the predominance of the amorphous structure of the composite hydrogel and the homogeneous distribution of GNPt within the network [46].

The surface morphology of the Gelatin/p(AETAC)/GNPt composite hydrogel (Gel 5) was characterized by SEM method. Figure 2c represents the porous structure of freeze-dried Gelatin/p(AETAC)/GNPt composite hydrogel (Gel 5) at 250× and 1000× magnifications. The presence of graphene nanoplates caused the hydrogel surface to appear wrinkled. When the SEM images were examined, it was determined that the Gel 5 had pores ranging from 50 µm to 300 µm.

The effect of the swelling ability of adsorbent materials such as hydrogel and composite hydrogel on adsorption is known [36]. Therefore, the effect of the amount of gelatin and the amount of GNPt on the swelling behavior of the composite hydrogel were investigated (Fig. 3a–d). In order to determine the effect of the amount of gelatin on the swelling behavior of the composite hydrogel, the equilibrium swelling values of the composite hydrogels prepared with varying amounts of gelatin in Table 1 are given in Fig. 3a. As seen in Fig. 3a, the swelling capacity of the composite hydrogel decreased with the increase in the amount of gelatin. The swelling capacities of the Gel 9, Gel 2, Gel 3, Gel 6, Gel 7 and Gel 8 composite hydrogels were 21.73 ± 0.73 g_{water}/g_{gel}, 21.61 ± 1.64 g_{water}/g_{gel}, 18.82 ± 0.81 g_{water}/g_{gel}, 17.24 ± 1.13 g_{water}/g_{gel}, 14.20 ± 0.51 g_{water}/g_{gel} and 13.96 ± 0.45 g_{water}/g_{gel}, respectively. This is thought to be related to the decrease in the ratio of AETAC, an ionic monomer, compared to the ratio of total monomer. The effect of the amount of GNPt in the composite hydrogel on the swelling behavior of composite hydrogels prepared with varying amounts of GNPt given in Table 1 and their swelling capacity was determined and given in Fig. 3b. The swelling capacities of the Gel 1, Gel 2, Gel 4 and Gel 5, composite hydrogels were 19.15 ± 1.93 g_{water}/g_{gel}, 21.61 ± 1.64 g_{water}/g_{gel}, 28.38 ± 1.29 g_{water}/g_{gel} and 48.22 ± 1.42 g_{water}/g_{gel}, respectively. It was determined that there was a significant increase in swelling capacity with the increase of GNPt content in the composite hydrogels. In addition, it was observed

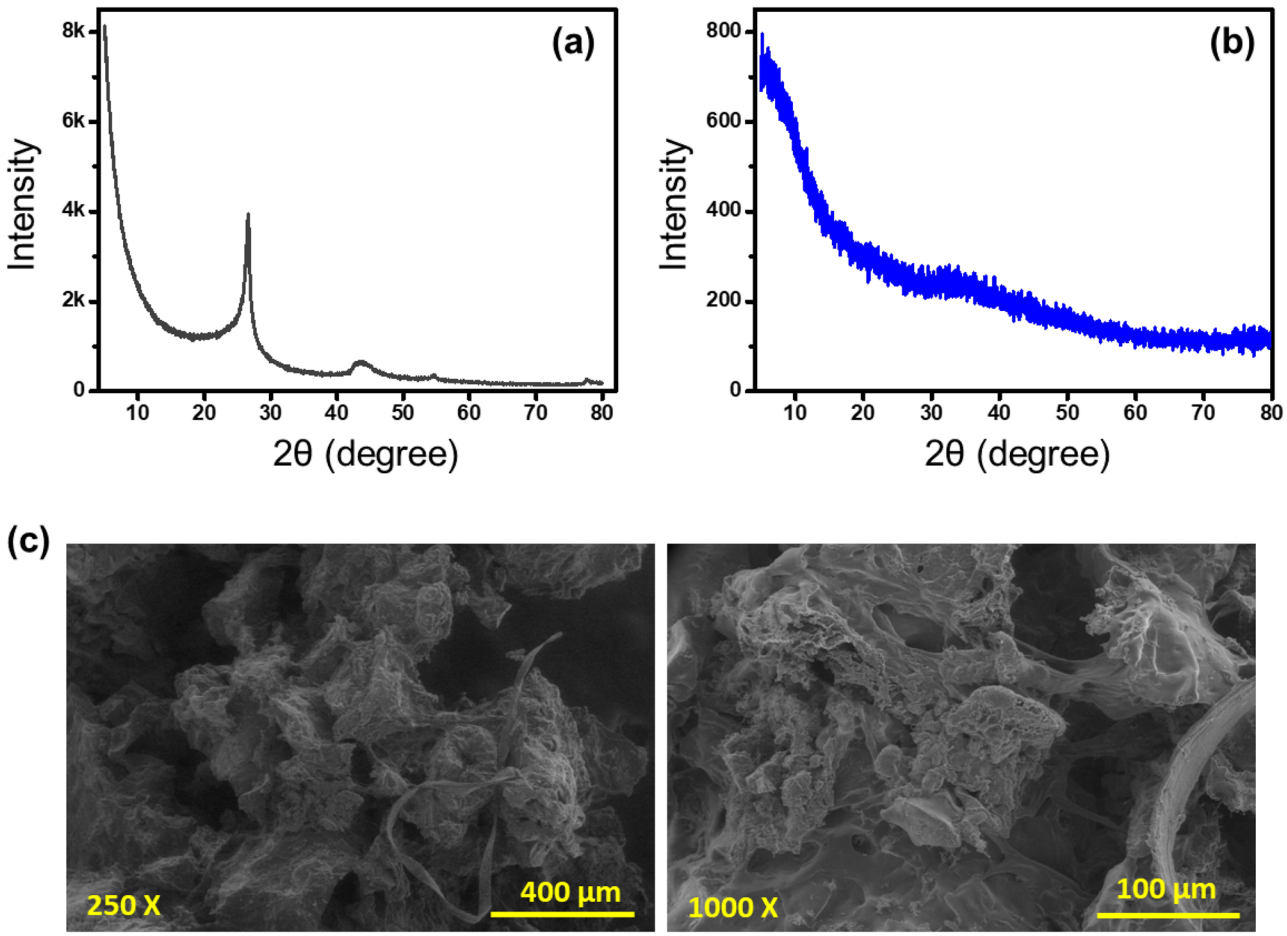

Fig. 2 **a** XRD spectra of GNPt and **b** Gelatin/p(AETAC)/GNPt composite hydrogel (Gel 5), and **c** SEM images of Gelatin/p(AETAC)/GNPt composite hydrogel (Gel 5)

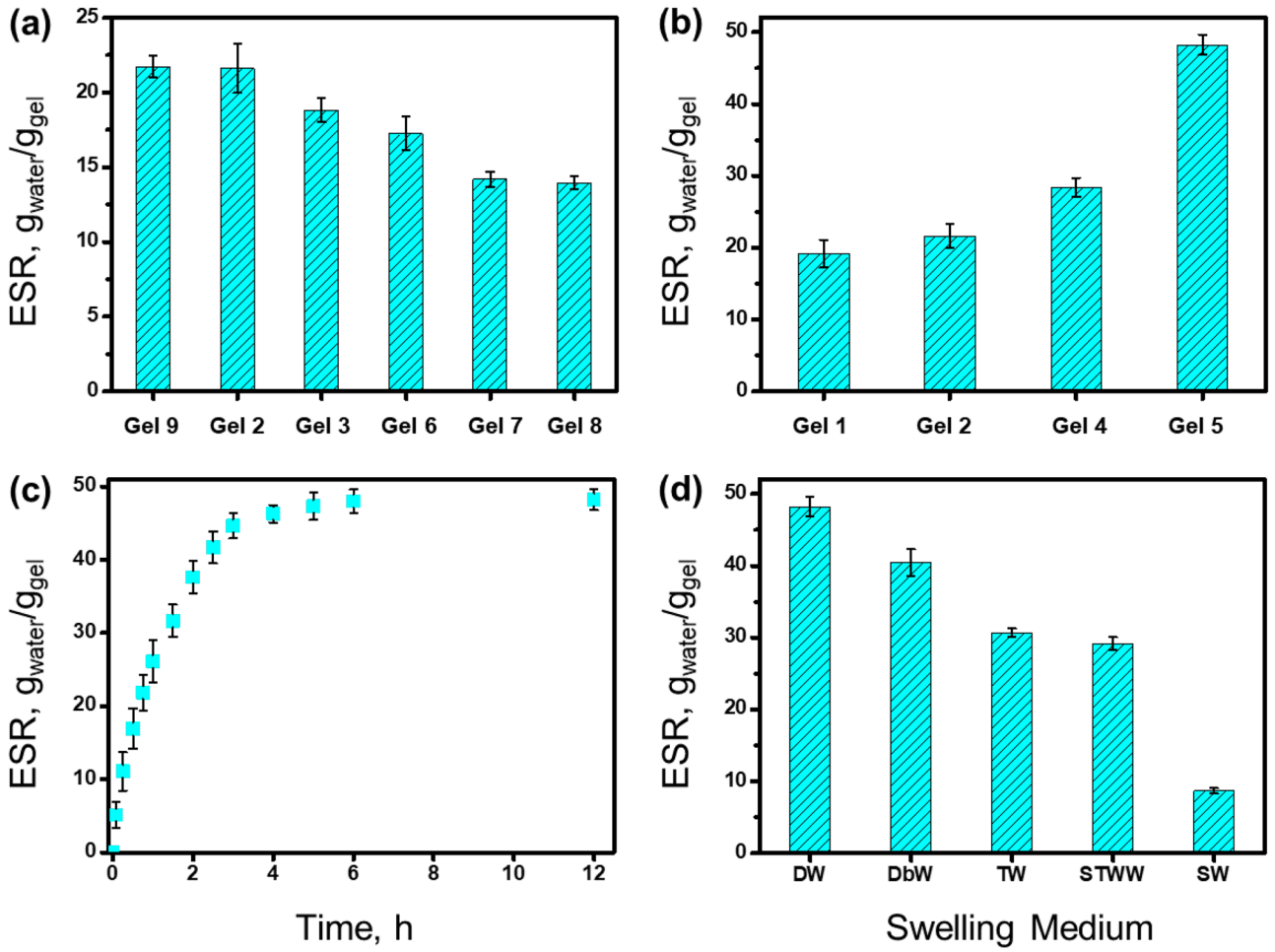

Fig. 3 Effect of **a** gelatin amount, **b** graphene nanoplate amount, **c** contact time (Gel 5) and **d** swelling medium (Gel 5) on swelling behavior of Gelatin/p(AETAC)/GNPt composite hydrogel

that the Gel 5 composite hydrogel did not disintegrate like other composite hydrogels in swelling capacity experiments. It has been reported in many studies that composite hydrogels prepared with materials such as bentonite and clay increase the durability and swelling capacity [16, 17, 21]. With the increase in the amount of GNPt, the durability of the composite hydrogel increases, and the structure of the composite hydrogel can be attributed to a more porous structure. The effects of contact time and different swelling mediums on the swelling behavior of Gel 5 composite hydrogel selected for use in the next experimental studies were investigated (Fig. 3c, d). As seen in Fig. 3c, Gel 5 composite hydrogel reached swelling capacity of 44.67 ± 1.77 g_{water}/g_{gel} at the 3 h. At the 6 h and 12 h, the swelling capacity was 48.01 ± 1.60 g_{water}/g_{gel} and 48.22 ± 1.42 g_{water}/g_{gel}, respectively. It was determined that the Gel 5 composite hydrogel reached the equilibrium swelling capacity in almost 3 h. Different swelling mediums can affect the swelling behavior of the composite hydrogel and therefore it is a parameter that can affect the adsorption ability of the adsorbent [14, 15]. For this reason, the swelling behavior of Gel 5 composite hydrogel in different water environments such as distilled water (DW), drinkable water (DbW), tap water (TW), synthetic textile wastewater (STWw), and seawater (SW) was investigated and shown in Fig. 3d. It was determined that the order of swelling capacities of Gel 5 composite hydrogel in different water mediums from largest to smallest is DW (48.22 ± 1.42 g_{water}/g_{gel}) > DbW (40.41 ± 1.89 g_{water}/g_{gel}) > TW (30.68 ± 0.56 g_{water}/g_{gel}) > STWw (29.19 ± 0.85 g_{water}/g_{gel}) > SW (8.66 ± 0.38 g_{water}/g_{gel}). Swelling capacity decreased in ion-rich water mediums. Also, the porosity value (50.01%) of the Gel 5 composite hydrogel, which has the highest swelling capacity among the composite hydrogels, also confirms its porosity. Such porous structures can facilitate the flow of dye molecules into the polymeric structure, which is important for developing materials with high adsorption capability. Considering all these results, Gel 5 composite hydrogel was chosen for dye adsorption studies.

Adsorption studies

Developing a material that can remove synthetic dyestuffs in industrial wastewater is important for sustainable water management. Adsorption experiments were carried out to determine the efficiency and optimum conditions of the prepared Gel 5 in removing synthetic dyes from wastewater.

The adsorption capacity of the Gel 5 is determined by its active surface sites and structural properties such as the charge and functional groups of organic dyes [47]. The interaction of Gel 5 with different dyes was carried out in anionic (ARS, MO and RB5) and cationic (MB, SO and MG) dye (Fig. S1) solutions with dye concentrations of 250 mg/L at 25 °C for 24 h. As seen in Fig. 4, the Gel 5 had a higher percentage of removal on anionic dyes than cationic dyes. The main reason for this situation was attributed to the interaction of AETAC, the cationic monomer in the Gel 5, and anionic dyes. At the same time, among the Gel 5 anionic dyes, the ARS dye molecule (90.72%) showed higher adsorption ability than the MO (69.32%) and RB5 (78.42%) dye molecules. ARS dye molecules, which have both hydroxyl groups and small sizes, can be effectively adsorbed on the surface-active sites of the Gel 5 [47]. In order to evaluate the adsorption efficiency for ARS dyestuff, in which Gel 5 has the highest percentage of dye removal, the effects of various parameters affecting adsorption such as initial dye concentration, adsorbent dose, contact time and temperature are discussed.

The effect of the initial concentration of ARS on the adsorption capacity of the Gel 5 was investigated in 30 ml dye solution prepared at different concentrations (25, 50, 100, 250, 500, 750 ve 1000 mg/L) (Fig. 5a) with 1 g/L adsorbent mass for 24 h at 25 °C. When Fig. 5a was examined, the percentage of dye removal of the Gel 5 was 90.37% at an initial concentration of 25 to 500 mg/L. The maximum ARS

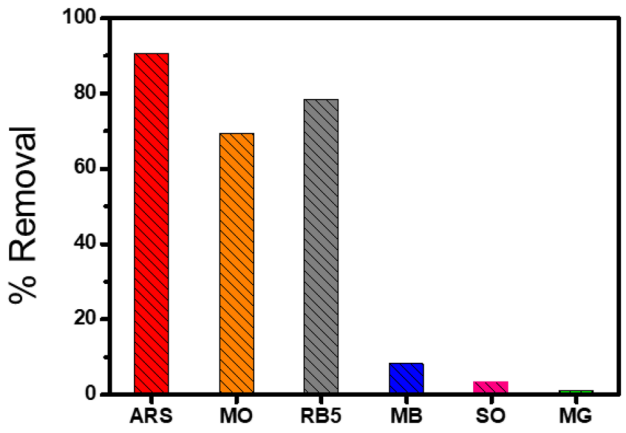

Fig. 4 Gelatin/p(AETAC)/GNPt composite hydrogel (Gel 5) for removal of various dyes (C_0 Dyes: 250 mg/L, 25 °C, 1 mL ARS Solution for 1 mg adsorbent and 24 h)

adsorption amount at the initial 500 and 1000 mg/L dye concentrations was 500.88 mg/g and 524.50 mg/g respectively. The dye adsorption capacity was decreased at solution concentrations higher than the initial concentration of 500 mg/L due to saturation of the adsorbent sites of the Gel 5 [18].

One of the most important parameters regulating the adsorption capacity at a fixed initial dye concentration is the amount of adsorbent [48]. The effect of the amount of Gel 5 on the adsorption ability was investigated in 30 ml dye solution with a dye concentration of 750 mg/L for 24 h at 25 °C. As shown in Fig. 5b, ARS dye removal increased from $57.56 \pm 0.74\%$ to $98.61 \pm 0.13\%$ by increasing the amount of Gel 5 from 0.5 g/L to 4 g/L. In general, as the amount of Gel 5 increases, the dye removal efficiency increases as there will be more active dye adsorption sites.

Another important factor examined is the effect of the contact time of the Gel 5 with the dye solution on the adsorption rate. Gel 5 (1 g/L) was analyzed in 30 ml of 500 mg/L ARS dye solution at 25 °C in a time interval of 15 min -24 h and the results are presented in Fig. 6a. With the increase in contact time, the Gel 5 increased the chance of interaction between hydrogel and dye molecules. However, after 6 h, the adsorption rate slowed down when the equilibrium between adsorbed dye molecules and adsorbent started to reach.

Since the pH value of wastewater can vary in a wide range, the pH of the solution can significantly affect the adsorption behavior of the adsorbent [49]. The effect of initial pH of ARS aqueous solutions was investigated using 1 g/L of Gel 5, 30 mL of the dye solution (250 mg/L) at different pH values ranging from 4 to 8 (4, 5, 6, 7, 8) at room temperature for 24 h (Fig. 6b). The dye removal percentages for the ARS dye solutions at pH 4, 5, 6, 7, and 8 of the Gel 5 were $90.54 \pm 0.98\%$, $89.71 \pm 1.12\%$, $90.84 \pm 0.15\%$, $87.27 \pm 1.09\%$, and $87.73 \pm 1.25\%$, respectively. The Gel 5 showed high ARS dye adsorption over a wide pH range. This may be related to the fact that the Gel 5 contains strongly ionized groups.

The temperature of the dye solution is one of the most important factors determining the adsorption capacity and yield by affecting the speed of dye molecules [50]. For the effect of temperature on adsorption, the maximum adsorption of the Gel 5 (1 g/L) in 750 mg/L ARS dye solution (30 mL) at different adsorption temperatures (25, 35, 45 and 55 °C) for 24 h was investigated (Fig. 7a). Equilibrium adsorption capacities at 25, 35, 45, and 55 °C temperatures were determined as 500.88 ± 10.61, 576.76 ± 14.45, 667.07 ± 8.96, and 706.41 ± 12.57 mg/g, respectively. It is clear from Fig. 7a that the adsorption capacity of Gel 5 increases as the temperature of the dye solution increases. With the increase in temperature, the mobility of ARS dye molecules increases and the viscosity of the solution decreases, thus facilitating the mobilization of the Gel 5 to the adsorbent sites [18, 51]. In addition, the obtained

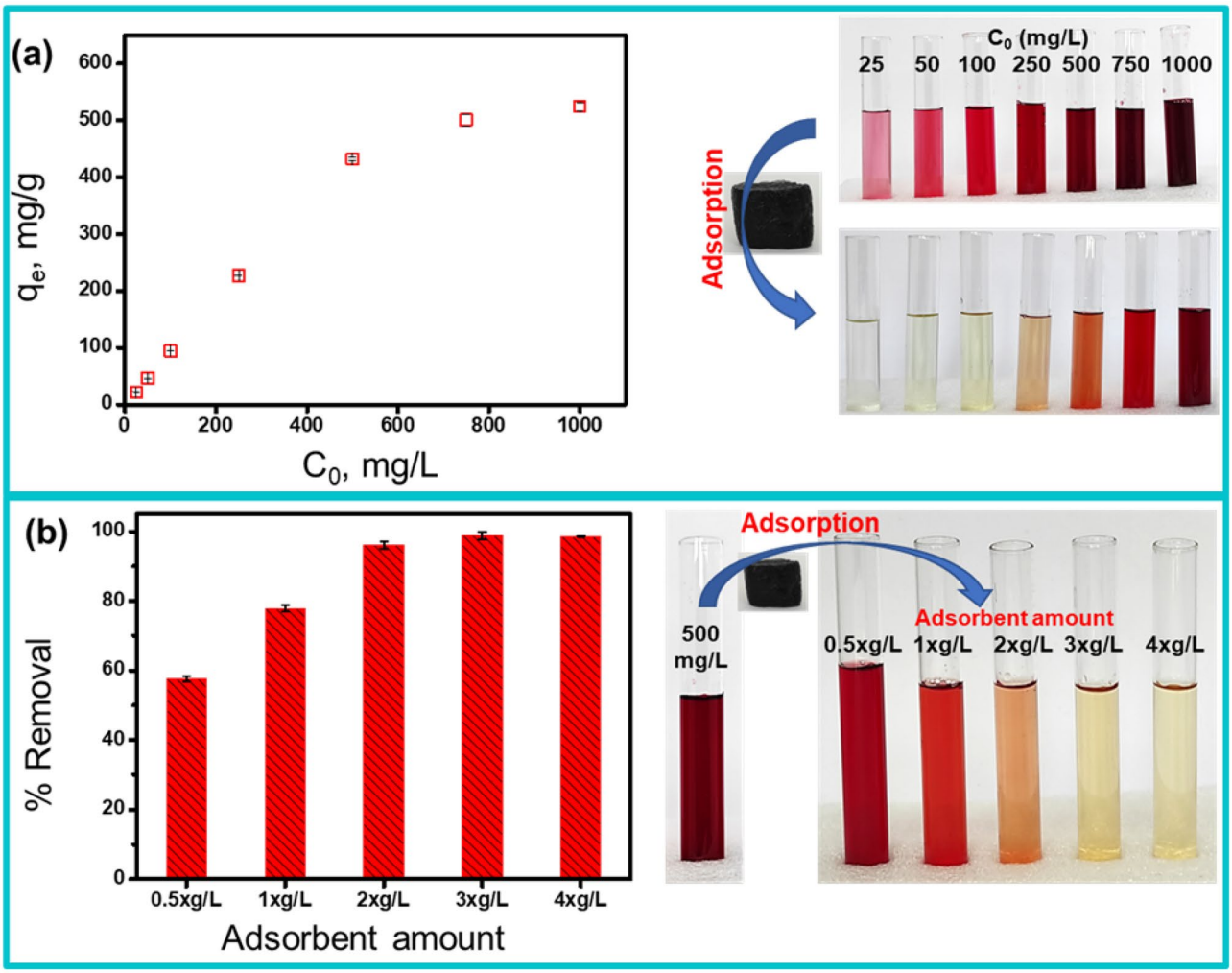

Fig. 5 Effect of **a** initial concentration (25 °C, 24 h and 1 mL ARS Solution for 1 mg adsorbent) and **b** adsorbent amount on ARS dye adsorption with Gelatin/p(AETAC)/GNPt composite hydrogel (Gel 5) (C_0 Dyes: 500 mg/L, 25 °C and 24 h)

data were used to calculate the thermodynamic parameters (Gibbs Free Energy – ΔG°, enthalpy – ΔH° and entropy – ΔS°) of the adsorbent that can guide its practical applications (Table 3). Thermodynamic parameters were calculated using the 1/T versus log (q_e/C_e) plot (Fig. 7b) [15].

ΔH° and ΔS° were determined with the help of the slope and intersection of the graph in Fig. 7b. The R^2 (0.98) value ΔH° and ΔS° of the linear graph in Fig. 7b represent the accuracy of the data [52]. As shown in Table 3, the ΔG° values at 25, 35, 45, and 55 °C were determined to be negative. This indicates that adsorption has spontaneous properties. ΔH° (52.89 ± 5.78 kj.mol^{-1}) and ΔS° (186.12 ± 18.57 j.mol^{-1}.K^{-1}) values were determined to be positive. A positive ΔH° value indicates an endothermic reaction, while a positive ΔS◦ value indicates the increase in randomness at the solid–liquid interface during the adsorption process.

Adsorption isotherm and kinetics

In order to investigate the adsorption performance of Gel 5, the equilibrium data of the adsorption of ARS dye molecules were simulated by linear Langmuir and Freundlich adsorption isotherm models, whose equations are given in Table S1 [16, 17]. Langmuir and Freundlich adsorption isotherm parameters were calculated from the slopes and intersections of the graphs in Fig. S2 obtained with these equations (Table 4). According to the data in Table 4, the ARS adsorption of Gel 5 conforms to the Langmuir model, which states that monolayer adsorption and adsorption sites are independent and uniform [36, 53].

In addition, the separation factor (R_L) values are in the range of 0 – 1 at all concentrations (Table 4). This indicates that the adsorption process between ARS and Gel 5 is suitable [16, 36].

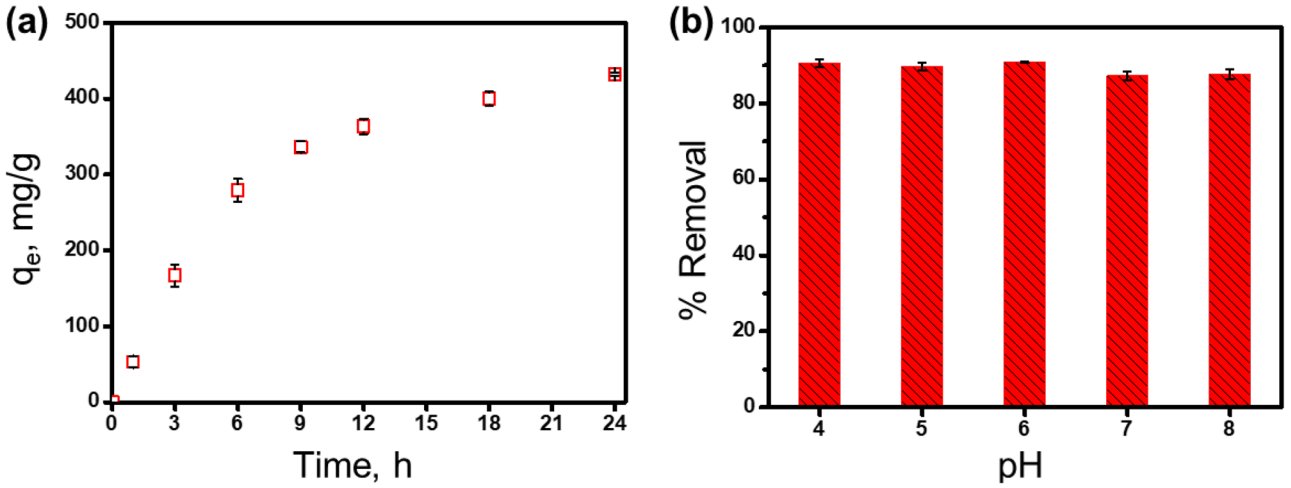

Fig. 6 Effect of **a** contact time (C_0 ARS: 500 mg/L, 25 °C and 1 mL ARS Solution for 1 mg adsorbent). and **b** pH of solution on ARS dye adsorption with Gelatin/p(AETAC)/GNPt composite hydrogel (Gel 5) (C_0 ARS: 250 mg/L, 25 °C, 1 mL ARS Solution for 1 mg adsorbent and 24 h)

PFO and PSO kinetic models were applied to investigate the adsorption mechanism of ARS dye molecules of Gel 5 [16, 54]. The graphs in Fig. S2c, d were created by using the linear PFO and PSO equations given in Table S1, and the slopes and intercepts obtained and the parameters of PFO and PSO were calculated and summarized in Table 4. When the experimental data were compared with the kinetic parameters in Table 4, the PSO model, which assumed that the adsorption rate was mainly limited by chemical adsorption, was more appropriate than the PFO model, which assumed that the adsorption rate was limited to the diffusion step [2].

To investigate the diffusion of ARS dye molecules into the pores of the Gel 5, it was analyzed with the aid of the graph in Fig. S2d, which was created with the linear intra-particle diffusion model given in Table S1 [16]. Obtained parameters are listed in Table 4. The size of the regression coefficient (R^2) and the value of C greater than zero indicate the contribution of surface adsorption [54]. All these results show that the adsorption of ARS dye molecules of the Gel 5 prepared is a chemical process that includes the intraparticle diffusion step.

Adsorption mechanism and performance

The adsorption process is greatly affected by the presence of both dye molecules and functional groups of the adsorbent [52]. In addition, the porosity of the adsorbent is another feature that affects the adsorption process [36]. The presence of carbonyl, hydroxyl, quaternized

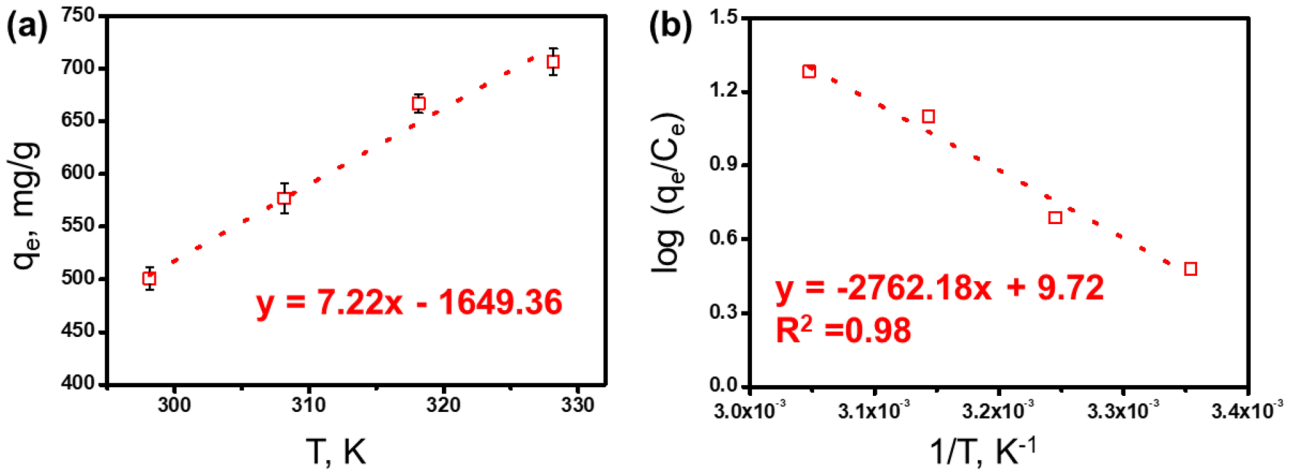

Fig. 7 **a** Effect of temperature on ARS dye adsorption with Gelatin/p(AETAC)/GNPt composite hydrogel (Gel 5) and **b** plot of 1/T vs. log (qe/Ce)

ammonium group, and aromatic ring in the structure of Gel 5 composite hydrogel together with the presence of hydroxyl, sulfonate, and aromatic rings in the structure of the ARS dye molecule can determine the adsorption process. The proposed adsorption mechanism for ARS anionic dye adsorption of Gel 5 composite hydrogel is given in Fig. 8. Gel 5 composite hydrogel creates an electrostatic interaction with the positively charged quaternized ammonium group in the composite hydrogel and the $–SO_3Na^+$ groups in the ARS dye molecules [2, 14]. Hydrogen bond interactions can occur with the hydroxyl groups of the ARS anionic dye molecule and the N and O atoms in the carbonyl, amine, hydroxyl, and sulfonate groups in the Gel 5 composite hydrogel structure [52]. In addition, the π – π stacking interaction between aromatic rings and the high porosity of the Gel 5 composite hydrogel favor dye adsorption, which facilitates the rapid migration of molecules [18, 52].

Table 3 Thermodynamic parameters for Gelatin/p(AETAC)/GNPt composite hydrogel (Gel5)

Thermodynamic Parameters	T (K)	ARS Dye
$\Delta H°$ (kj.mol^{-1})		52.89 ± 5.78
$\Delta S°$ (j.mol^{-1}.K^{-1})		186.12 ± 18.57
$\Delta G°$ (kj.mol^{-1})	298.15 K	-2.60
	308.15 K	-4.46
	318.15 K	-6.32
	328.15 K	-8.18

The ARS removal of Gel 5 used in this study and some adsorbents in the literature is summarized in Table 5. When

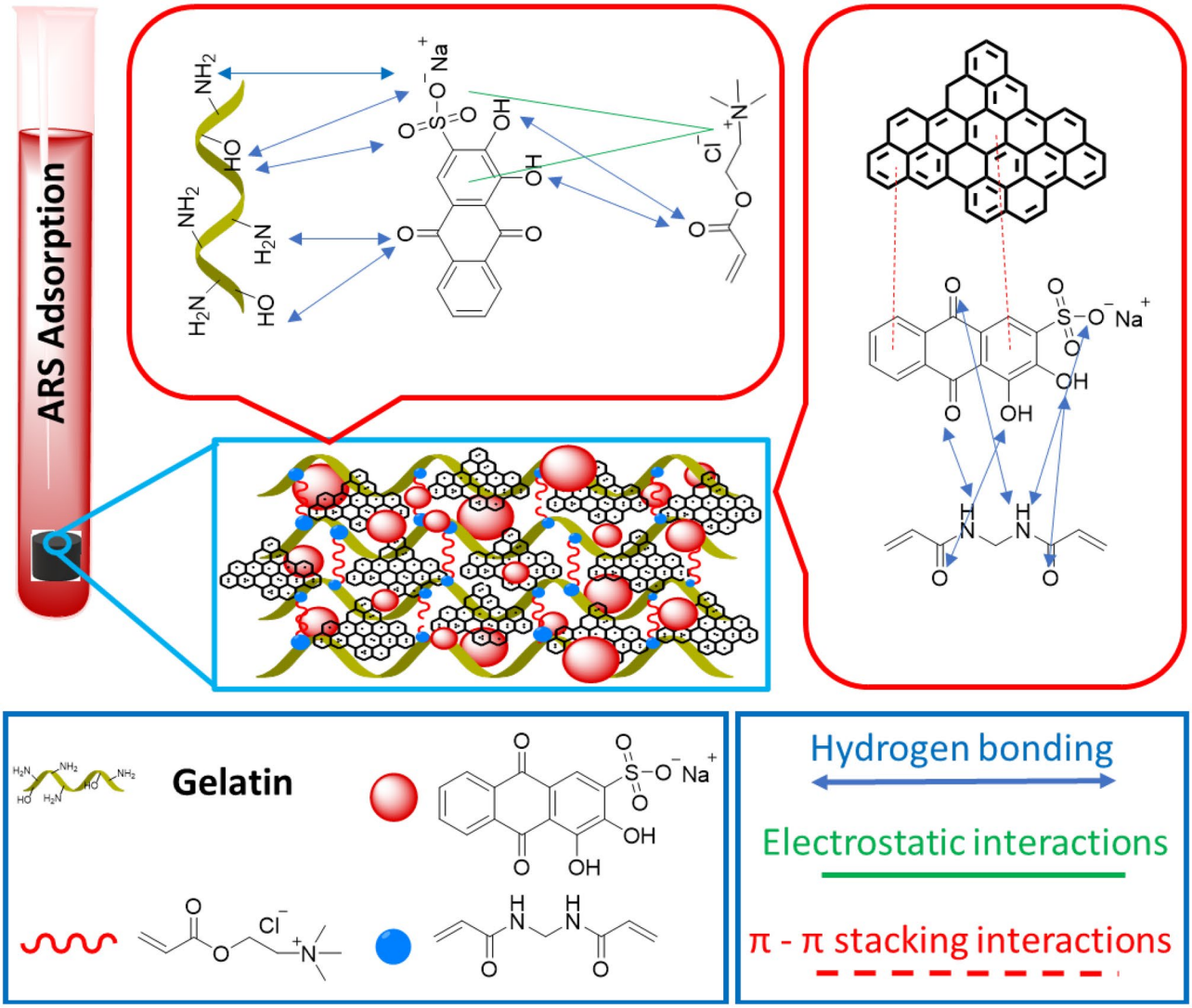

Fig. 8 Illustration of the predicted mechanism of ARS dye adsorption by Gelatin/p(AETAC)/GNPt composite hydrogel (Gel 5)

Table 4 Isotherm and kinetic parameters for Gelatin/p(AETAC)/GNPt composite hydrogel (Gel5)

Isotherms and Kinetics	Isotherm Models		Kinetic Models		
	Langmuir	Freundlich	PFO	PSO	Intra-particle diffusion
q_m (mg.g^{-1})	649.35				
K_L (L.mg^{-1})	0.0199				
R_L	0.05–0.67				
K_f (mg.g^{-1})		0.0514			
n		2.97			
q_e (mg.g^{-1})			588.84	512.82	
k_1 (h^{-1})			0.22		
k_2 (g.mg^{-1}.h^{-1})				4.02×10^{-4}	
C					96.45
k_i (mg.g^{-1}.h$^{-0.5}$)					3.42
R_i					0.99
R^2	0.97	0.65	0.90	0.93	0.95

the table is examined, Gel 5 has a higher adsorption performance than other adsorbents. All these data show that Gel 5 is an efficient material for dye removal activities from anionic dye-containing wastewater.

Reusability of composite hydrogel

The reusability of adsorbent systems is one of the important parameters in terms of both sustainability and efficiency. For this reason, the adsorption–desorption study of the Gel 5 composite hydrogel was carried out. The percentage of ARS dye removal for 3 cycles of the composite hydrogel was found to be 93.31%, 79.85%, and 68.57%, respectively. The decrease in the adsorption efficiency of Gel 5 can be attributed to the weakening of the electrostatic interaction between the composite hydrogel and the ARS dye with each use [37]. These results show that the ARS dyestuff of gel 5 can be recycled and the composite hydrogel can be reused.

Mechanical strength is one of the important factors for the reusability of adsorbents. For this reason, the durability of the composite hydrogel was investigated by a mechanical compression test. In Fig. 9a, it can be seen that the composite hydrogel is dry, swollen, adsorbed by ARS, and retains its form in the post-desorption photographs. At the same time, it is seen that the composite hydrogel prepared in Fig. 9a has a flexible structure. Figure 9b, c show the mechanical test results and images of the pre-adsorption and post-desorption composite hydrogel. As it is known, graphene is a material with high mechanical strength and increases the durability of the structure [58]. In hydrogels containing GNPt, it is expected that the mechanical properties of graphene will be high due to this property [59]. Thus, the GNpt in the Gel 5 composite hydrogel and the crosslinker MBA showed very good mechanical properties. It is thought that GNpt are incorporated into the structure wrapped around their pore walls and thus support cross-links. In this way, it can be stated that the mechanical strength of the composite hydrogel increases. In addition, 199.64 kPa compressive strength was observed for 50% strain before the desorption of Gel 5 composite hydrogel, while 194.29 kPa compressive strength was observed post-desorption. When the pre-adsorption and post-desorption composite hydrogel are compared, it is clearly seen that there is no significant difference between the compressive strengths. This shows that the composite

Table 5 Comparison of different adsorbents in the literature for ARS dye removal

Adsorbents	q_m (mg.g^{-1})	Best fit isotherm	References
Coal bottom ash derived zeolite	210.75	Langmuir	[2]
Schima wallichii activated carbon	91.965	Langmuir	[52]
Activated carbon/γ-Fe_2O_3 nano-composite	108.69	Langmuir	[55]
Calcium phosphate hydroxyapatite	100.36	Sips and Dubinin–Radushkevich	[56]
Fe_3O_4@NiO core–shell magnetic nanoparticles	223.30	Freundlich	[1]
APTES grafted silica	59.8	Langmuir	[57]
Gelatin/p(AETAC)/GNPt (Gel5)	649.35	Langmuir	**In this study**

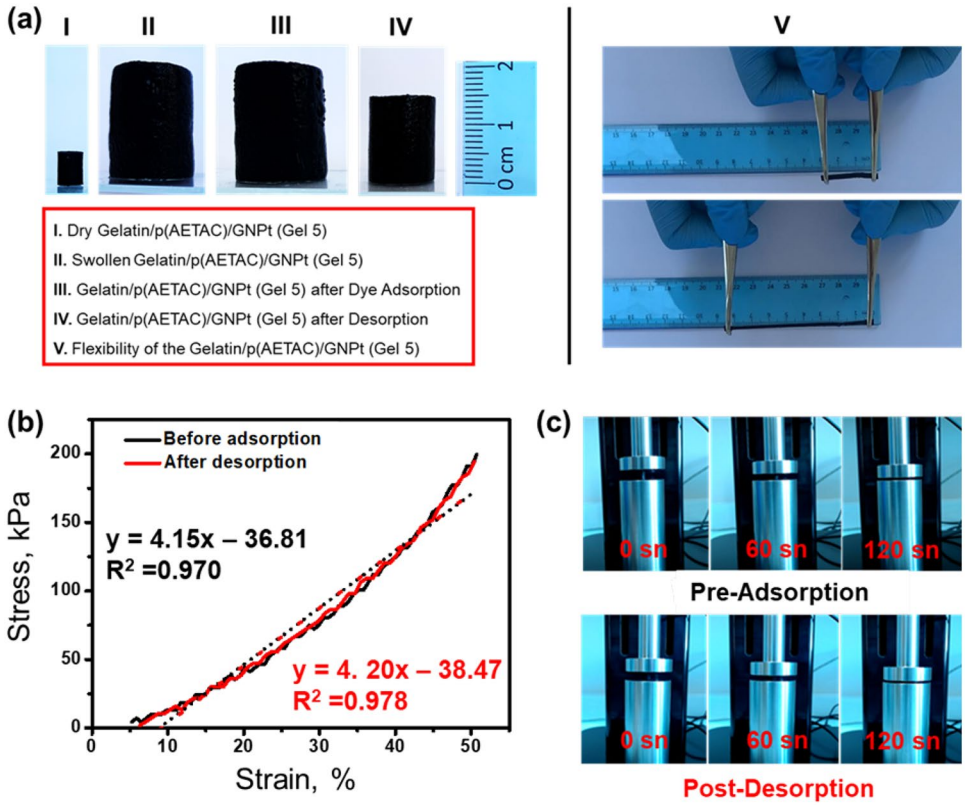

Fig. 9 **a** Dry, swollen, ARS adsorbed, post-desorption and flexibility images of the Gelatin/p(AETAC)/GNPt composite hydrogel (Gel 5), **b** Compressive stress–strain graphs and **c** images of the Gelatin/p(AETAC)/GNPt composite hydrogel (Gel 5) pre-adsorption and post-desorption

hydrogel does not lose its mechanical properties after dye absorption and desorption processes and has reusability. These results support each other with similar studies in the literature [60].

Conclusion

Gelatin/p(AETAC)/GNPt composite hydrogel containing porous Graphene nanoplate with high adsorption efficiency in a wide pH range was successfully prepared by the free-radical copolymerization method. The biocompatible, porous composite hydrogel containing Graphene nanoplate has high efficiency in removing ARS anionic dye from water. Adsorption and equilibrium parameters, which are important parameters in the transition from laboratory scale to large scale, were determined by adsorption experiments. Adsorption data are compatible with the Langmuir isotherm and PSO kinetic model. ARS adsorption of Gelatin/p(AETAC)/GNPt composite hydrogel is a chemical process that includes an intraparticle diffusion step. In addition, the composite hydrogel had mechanical strength, which is an important parameter for reusability. The results showed that Gelatin/p(AETAC)/GNPt composite hydrogel can be used as an efficient adsorbent for the removal of anionic dyestuffs from wastewater.

Supplementary Information The online version contains supplementary material available at https://doi.org/10.1007/s10965-022-03327-5.

Acknowledgements There is no financial support. We thank Çanakkale Onsekiz Mart University Science and Technology Application and Research Center (COBILTUM) and Namık Kemal University Central Research Laboratory (NABILTEM) for characterization analyses. We thank Associate Professor Yavuz Emre Arslan for the mechanical compression analyses.

Authors contributions All authors contributed to the study conception and design. Material preparation, data collection and analysis were performed by [Fatma Ozsoy], [Batuhan Ozdilek], [Alper Onder] [Pinar Ilgin], [Hava Ozay] and [Ozgur Ozay]. The first draft of the manuscript was written by [Fatma Ozsoy], [Batuhan Ozdilek] and [Alper Onder]. All authors commented on previous versions of the manuscript. All authors read and approved the final manuscript.

Data availability All data generated or analyzed during this study are included in this published article and its supplementary information files.

Declarations

Ethical approval This article does not contain any studies with human participants or animals performed by any of the authors.

Informed consent Informed consent was obtained from all individual participants included in the study.

Conflict of interest The authors declare that they have no conflict of interest.

References

1. Nodehi R, Shayesteh H, Rahbar-Kelishami A (2021) Fe_3O_4@NiO core–shell magnetic nanoparticle for highly efficient removal of Alizarin red S anionic dye. Int J Environ Sci Technol. https://doi.org/10.1007/s13762-021-03399-8
2. Gollakota ARK, Munagapati VS, Volli V, Gautam S, Wen JC, Shu CM (2021) Coal bottom ash derived zeolite (SSZ-13) for the sorption of synthetic anion Alizarin Red S (ARS) dye. J Hazard Mater 416:125925. https://doi.org/10.1016/j.jhazmat.2021.125925
3. Gul A, Muhammad S, Nawaz S, Munir S, Rehman KU, Ahmad S, Humphrey OS (2021) Ficus religiosa bark an efficient adsorbent for Alizarin Red S dye: Equilibrium and kinetic analysis. J Iran Chem Soc. https://doi.org/10.1007/s13738-021-02413-7
4. Lu W, Chen N, Feng C, Deng Y, Zhang J, Chen F (2020) Treatment of polluted river sediment by electrochemical oxidation: Changes of hydrophilicity and acute cytotoxicity of dissolved organic matter. Chemosphere 243:125283. https://doi.org/10.1016/j.chemosphere.2019.125283
5. Liu Y, Liu H, Shen Z (2021) Nanocellulose based filtration membrane in industrial waste water treatment: A review. Materials (Basel). https://doi.org/10.3390/ma14185398
6. Liu Y, Zhang J, Huang H, Huang Z, Xu C, Guo G, He H, Ma J (2019) Treatment of trace thallium in contaminated source waters by ferrate pre-oxidation and poly aluminium chloride coagulation. Sep Purif Technol 227:115663. https://doi.org/10.1016/j.seppur.2019.06.001
7. Natarajan S, Bajaj HC, Tayade RJ (2018) Recent advances based on the synergetic effect of adsorption for removal of dyes from waste water using photocatalytic process. J Environ Sci (China) 65:201–222. https://doi.org/10.1016/j.jes.2017.03.011
8. Janani R, Gurunathan B, Sivakumar K, Varjani S, Ngo HH, Gnansounou E (2022) Advancements in heavy metals removal from effluents employing nano-adsorbents: Way towards cleaner production. Environ Res 203:111815. https://doi.org/10.1016/j.envres.2021.111815
9. de Azevedo ACN, Vaz MG, Gomes RF, Pereira AGB, Fajardo AR, Rodrigues FHA (2017) Starch/rice husk ash based superabsorbent composite: high methylene blue removal efficiency. Iran Polym J 26(2):93–105. https://doi.org/10.1007/s13726-016-0500-2
10. Ghawanmeh AA, Ali GAM, Algarni H, Sarkar SM, Chong KF (2019) Graphene oxide-based hydrogels as a nanocarrier for anticancer drug delivery. Nano Res 12(5):973–990. https://doi.org/10.1007/s12274-019-2300-4
11. Weng M, Zhu Q, Wang A, Liu G, Huang H (2020) A new type of SnO_2@β-Fe(Zr)OOH hollow nanosphere as a bifunctional adsorbent for removing nitrate from water: kinetics, isotherm, and thermodynamic studies. J Mater Sci 55(33):15797–15812. https://doi.org/10.1007/s10853-020-05142-z
12. Shan W, Du J, Yang K, Ren T, Wan D, Pu H (2021) Superhydrophobic and superoleophilic polystyrene/carbon nanotubes foam for oil/water separation. J Environ Chem Eng 9(5):106038. https://doi.org/10.1016/j.jece.2021.106038
13. Zhu W, Han M, Kim D, Zhang Y, Kwon G, You J, Jia C, Kim J (2022) Facile preparation of nanocellulose/Zn-MOF-based catalytic filter for water purification by oxidation process. Environ Res 205:112417. https://doi.org/10.1016/j.envres.2021.112417
14. Onder A, Ilgin P, Ozay H, Ozay O (2020) Removal of dye from aqueous medium with pH-sensitive poly[(2-(acryloyloxy)ethyl] trimethylammonium chloride-co-1-vinyl-2-pyrrolidone] cationic hydrogel. J Environ Chem Eng 8(5):104436. https://doi.org/10.1016/j.jece.2020.104436
15. Onder A, Ilgin P, Ozay H, Ozay O (2021) Preparation of composite hydrogels containing fly ash as low-cost adsorbent material and its use in dye adsorption. Int J Environ Sci Technol. https://doi.org/10.1007/s13762-021-03622-6
16. Jiang M, Niu N, Chen L (2021) A template synthesized strategy on bentonite-doped lignin hydrogel spheres for organic dyes removal. Sep Purif Technol 285:120376. https://doi.org/10.1016/j.seppur.2021.120376
17. Baigorria E, Fraceto LF (2022) Novel nanostructured materials based on polymer/organic-clay composite networks for the removal of carbendazim from waters. J Clean Prod 331:129867. https://doi.org/10.1016/j.jclepro.2021.129867
18. Mani SK, Bhandari R (2022) Microwave-assisted synthesis of self-assembled network of Graphene oxide-Polyethylenimine-Polyvinyl alcohol hydrogel beads for removal of cationic and anionic dyes from wastewater. J Mol Liq 345:117809. https://doi.org/10.1016/j.molliq.2021.117809
19. Wang R, Yu Q, He Y, Bai J, Jiao T, Zhang L, Bai Z, Zhou J, Peng Q (2019) Self-assembled polyelectrolyte-based composite hydrogels with enhanced stretchable and adsorption performances. J Mol Liq 294:111576. https://doi.org/10.1016/j.molliq.2019.111576
20. Gad YH, Nasef SM (2021) Radiation synthesis of graphene oxide/composite hydrogels and their ability for potential dye adsorption from wastewater. J Appl Polym Sci 138(41):1–19. https://doi.org/10.1002/app.51220
21. Gao B, Yu H, Wen J, Zeng H, Liang T, Zuo F, Cheng C (2021) Super-adsorbent poly(acrylic acid)/laponite hydrogel with ultrahigh mechanical property for adsorption of methylene blue. J Environ Chem Eng 9(6):106346. https://doi.org/10.1016/j.jece.2021.106346
22. Hu W, Zhang P, Liu X, Yan B, Xiang L, Zhang J, Gong L, Huang J, Cui K, Zhu L, Zeng H (2018) An amphiphobic graphene-based hydrogel as oil-water separator and oil fence material. Chem Eng J 353:708–716. https://doi.org/10.1016/j.cej.2018.07.147
23. Meng X, Lu L, Sun C (2018) Green Synthesis of Three-Dimensional MnO_2/Graphene Hydrogel Composites as a High-Performance Electrode Material for Supercapacitors. ACS Appl Mater Interfaces 10(19):16474–16481. https://doi.org/10.1021/acsami.8b02354
24. Durmuş S, Yilmaz B, Kıvanç MR, Onder A, Ilgin P, Ozay H, Ozay O (2021) Synthesis, characterization, and in vitro drug release properties of AuNPs/p(AETAC-co-VI)/Q nanocomposite hydrogels. Gold Bull. https://doi.org/10.1007/s13404-021-00295-4
25. Ren J, Wang X, Zhao L, Li M, Yang W (2022) Double network gelatin/chitosan hydrogel effective removal of dyes from aqueous solutions. J Polym Environ 30:2007–2021. https://doi.org/10.1007/s10924-021-02327-8
26. Bang S, Jung UW, Noh I (2018) Synthesis and biocompatibility characterizations of in situ chondroitin sulfate-gelatin hydrogel for tissue engineering. Tissue Eng Regen Med 15(1):25–35. https://doi.org/10.1007/s13770-017-0089-3
27. Lee Y, Yim S, Lee GW, Kim S, Kim HS, Hwang DY, An B, Lee JH, Seo S, Yang SY (2020) Self-adherent biodegradable gelatin-based hydrogel electrodes for electrocardiography monitoring. Sensors (Switzerland) 20(20):1–12. https://doi.org/10.3390/s20205737
28. Nazeri MT, Javanbakht S, Shaabani A, Ghorbani M (2020) 5-aminopyrazole-conjugated gelatin hydrogel: A controlled 5-fluorouracil delivery system for rectal administration. J Drug Deliv Sci Technol 57:1–8. https://doi.org/10.1016/j.jddst.2020.101669
29. Faghihi S, Gheysour M, Karimi A, Salarian R (2014) Fabrication and mechanical characterization of graphene oxide-reinforced poly (acrylic acid)/gelatin composite hydrogels. J Appl Phys 115:083513. https://doi.org/10.1063/1.4864153
30. Zheng X, Zhang Q, Liu J, Pei Y, Tang K (2016) A unique high mechanical strength dialdehyde microfibrillated cellulose/gelatin composite hydrogel with a giant network structure. RSC Adv 6:71999. https://doi.org/10.1039/c6ra12517d
31. Ganguly S, Das NC (2015) Synthesis of a novel pH responsive phyllosilicate loaded polymeric hydrogel based on poly(acrylic

acid-co-N-vinylpyrrolidone) and polyethylene glycol for drug delivery: Modelling and kinetics study for the sustained release of an antibiotic drug. RSC Adv 5(24):18312–18327. https://doi.org/10.1039/c4ra16119j
32. Yao G, Liu X, Zhang G, Han Z, Liu H (2021) Green synthesis of tannic acid functionalized graphene hydrogel to efficiently adsorb methylene blue. Colloids Surfaces A Physicochem Eng Asp 625:126972. https://doi.org/10.1016/j.colsurfa.2021.126972
33. Ren J, Wang X, Zhao L, Li M, Yang W (2021) Effective removal of dyes from aqueous solutions by a gelatin hydrogel. J Polym Environ 29(11):3497–3508. https://doi.org/10.1007/s10924-021-02136-z
34. Li K, Yan J, Zhou Y, Li B, Li X (2021) β-cyclodextrin and magnetic graphene oxide modified porous composite hydrogel as a superabsorbent for adsorption cationic dyes: Adsorption performance, adsorption mechanism and hydrogel column process investigates. J Mol Liq 335:116291. https://doi.org/10.1016/j.molliq.2021.116291
35. Patel SR, Patel MP (2021) Green and facile preparation of ultrasonic wave-assisted chitosan-g-poly-(AA/DAMPB)/Fe_3O_4 composite hydrogel for sequestration of reactive black 5 dye. Polym Bull. https://doi.org/10.1007/s00289-021-03662-5
36. Kıvanç MR, Ozay O, Ozay H, Ilgin P (2020) Removal of anionic dyes from aqueous media by using a novel high positively charged hydrogel with high capacity. J Dispers Sci Technol. https://doi.org/10.1080/01932691.2020.1847658
37. Gautam RK, Gautam PK, Chattopadhyaya MC et al (2014) Adsorption of Alizarin Red S onto biosorbent of Lantana camara: kinetic, equilibrium modeling and thermodynamic studies. Proc Natl Acad Sci India Sect A Phys Sci 84:495–504. https://doi.org/10.1007/s40010-014-0154-4
38. Bukhari SMH, Khan S, Rehanullah M, Ranjha NM (2015) Synthesis and characterization of chemically cross-linked acrylic acid/gelatin hydrogels: effect of pH and composition on swelling and drug release. Int J Polym Sci. https://doi.org/10.1155/2015/187961
39. Xing Q, Yates K, Vogt C et al (2014) Increasing mechanical strength of gelatin hydrogels by divalent metal ion removal. Sci Rep 4:4706. https://doi.org/10.1038/srep04706
40. Olivero RA, Nocerino JM, Deming SN (1995) Experimental design and optimization. Handb Environ Chem 2:73–122. https://doi.org/10.1007/978-3-540-49148-4_3
41. Putri TS, Ratnasari A, Sofiyaningsih N, Nizar MS, Yuliati A, Shariff KA (2022) Mechanical improvement of chitosan–gelatin scaffolds reinforced by β-tricalcium phosphate bioceramic. Ceram Int. https://doi.org/10.1016/j.ceramint.2021.12.367
42. Wang H, Lu W, Ke L, Wang Y, Zhou J, Rao P (2022) Effect of hydroxychloroquine sulfate on the gelation behavior, water mobility and structure of gelatin. Colloids Surf A Physicochem Eng Asp 633(P2):127849. https://doi.org/10.1016/j.colsurfa.2021.127849
43. Chen Y, Zhang H, Xu C, Cong R, Fang G (2022) Thermal properties of 1-hexadecanol/high density polyethylene/graphene nanoplates composites as form-stable heat storage materials. Sol Energy Mater Sol Cells 237:111580. https://doi.org/10.1016/j.solmat.2022.111580
44. Guo Z, Ren P, Zhang Z, Dai Z, Lu Z, Jin Y, Ren F (2022) Fabrication of carbonized spent coffee grounds/graphene nanoplates/cyanate ester composites for superior and highly absorbed electromagnetic interference shielding performance. J Mater Sci Technol 102:123–131. https://doi.org/10.1016/j.jmst.2021.05.082
45. Aziz SN, Abid SA, Al-Alak SK, Al Kadmy IMS, Rheima AM (2022) Spread of ESβL-producing Escherichia coli and the anti-virulence effect of graphene nano-sheets. Arch Microbiol 204(1):1–8. https://doi.org/10.1007/s00203-021-02687-8
46. Luo H, Dong J, Xu X, Wang J, Yang Z, Wan Y (2018) Exploring excellent dispersion of graphene nanosheets in three-dimensional bacterial cellulose for ultra-strong nanocomposite hydrogels. Compos A Appl Sci Manuf 109:290–297. https://doi.org/10.1016/j.compositesa.2018.03.007
47. Joshi P, Sharma OP, Ganguly SK, Srivastava M, Khatri OP (2022) Fruit waste-derived cellulose and graphene-based aerogels: Plausible adsorption pathways for fast and efficient removal of organic dyes. J Colloid Interface Sci 608:2870–2883. https://doi.org/10.1016/j.jcis.2021.11.016
48. Xu S, Jin Y, Li R, Shan M, Zhang Y (2022) Amidoxime modified polymers of intrinsic microporosity/alginate composite hydrogel beads for efficient adsorption of cationic dyes from aqueous solution. J Colloid Interface Sci 607:890–899. https://doi.org/10.1016/j.jcis.2021.08.157
49. Wu Z, Zhang P, Zhang H, Li X, He Y, Qin P, Yang C (2022) Tough porous nanocomposite hydrogel for water treatment. J Hazard Mater 421:126754. https://doi.org/10.1016/j.jhazmat.2021.126754
50. Wang M, Li Y, Cui M, Li M, Xu W, Li L, Sun Y, Chen B, Chen K, Zhang Y (2021) Barium alginate as a skeleton coating graphene oxide and bentonite-derived composites: excellent adsorbent based on predictive design for the enhanced adsorption of methylene blue. J Colloid Interface Sci 611:629–643. https://doi.org/10.1016/j.jcis.2021.12.115
51. Bayram T, Bucak S, Ozturk D (2020) BR13 dye removal using sodium dodecyl sulfate modified montmorillonite: Equilibrium, thermodynamic, kinetic and reusability studies. Chem Eng Process - Process Intensif 158:108186. https://doi.org/10.1016/j.cep.2020.108186
52. Bhomick PC, Supong A, Baruah M, Pongener C, Gogoi C, Sinha D (2020) Alizarin Red S adsorption onto biomass-based activated carbon: optimization of adsorption process parameters using Taguchi experimental design. Int J Environ Sci Technol 17:1137. https://doi.org/10.1007/s13762-019-02389-1
53. Jiang X, Ding W, Li H, Zhang Z, Zhong Z, Liu H, Zheng H (2022) Facile synthesis of Poly(epichlorohydrin-diethylenetriamine) hydrogel for highly selective diclofenac sodium removal. Sep Purif Technol 283:120215. https://doi.org/10.1016/j.seppur.2021.120215
54. Darwisha AAA, Rashada M, AL-Aoh HA (2019) Methyl orange adsorption comparison on nanoparticles: Isotherm, kinetics, and thermodynamic studies. Dyes Pigments 160:563. https://doi.org/10.1016/j.dyepig.2018.08.045
55. Fayazi M, Ghanei-Motlagh M, Taher MA (2015) The adsorption of basic dye (Alizarin red S) from aqueous solution onto activated carbon/γ-Fe_2O_3 nano-composite: Kinetic and equilibrium studies. Mater Sci Semicond 40:35. https://doi.org/10.1016/j.mssp.2015.06.044
56. Adeogun AI, Babu RB (2021) One-step synthesized calcium phosphate-based material for the removal of alizarin S dye from aqueous solutions: isothermal, kinetics, and thermodynamics studies. Appl Nanosci 11:1–13. https://doi.org/10.1007/s13204-015-0484-9
57. Ali N, Ali F, Ullah I, Ali Z, Duclaux L, Reinert L, Lévêque JM, Farooq A, Bilal M, Ahmad I (2020) Organically modified micron-sized vermiculite and silica for efficient removal of Alizarin Red S dye pollutant from aqueous solution. Environ Technol Innov 19:101001. https://doi.org/10.1016/j.eti.2020.101001
58. Yan X et al (2018) Mechanical properties of gelatin/polyacrylamide/graphene oxide nanocomposite double-network hydrogels. Compos Sci Technol 163:81–88. https://doi.org/10.1016/j.compscitech.2018.05.011
59. Pan C, Liu L, Chen Q, Zhang Q, Guo G (2017) Tough, stretchable, compressive novel polymer/graphene oxide nanocomposite hydrogels with excellent self-healing performance. ACS Appl Mater Interfaces 9(43):38052–38061. https://doi.org/10.1021/acsami.7b12932

60. Nazar V, Kashi M, Haghbin Nazarpak M, Shahryari E, Mehrjoo M (2022) Gelatin hydrogel reinforced by graphene oxide grafted chitosan for cartilage tissue engineering application. Int J Polym Mater Polym Biomater. https://doi.org/10.1080/00914037.2022.2085704